Proceedings of the 2002 IEEE
International Conference on Robotics & Automation
Washington, DC • May 2002

Dynamic Scaling of Trajectories for Robots with Elastic Joints *

Alessandro De Luca Riccardo Farina

Dipartimento di Informatica e Sistemistica
Università degli Studi di Roma "La Sapienza"
Via Eudossiana 18, 00184 Roma, Italy
deluca@dis.uniroma1.it

Abstract

The classical dynamic scaling property of robot trajectories is analyzed in the case of presence of elastic transmissions. We present a technique for recovering the fastest motion under torque constraints, when uniform time scaling is used along a given path. The scaling algorithm is based on the solution of a complete quartic polynomial equation, which reduces to a biquadratic one in the absence of viscous friction. Consequences on the organization of inverse dynamics computation are pointed out. Numerical results are reported for a planar 2R arm, illustrating the differences that arise with respect to the fully rigid case.

1 Introduction

Robot trajectories are often formulated in terms of a parametrized path in the cartesian or joint space and of an associated timing law. This convenient decomposition allows to redesign the timing law, e.g., for speeding up or slowing down the overall motion time, without affecting the actual geometric path [1].

A fundamental property of time scaling of trajectories for the dynamic model of rigid robots was independently pointed out by Bobrow [2] and Hollerbach [3]. When the traveling time along a geometric path is uniformly scaled by a factor λ, the torque needed for executing the new trajectory is scaled by a factor λ^2, up to the gravitational torque contribution. This allows to locally optimize the available torque range or to recover from unfeasible torques violating the actuator constraints, without the need of performing again inverse dynamics computation [4]. The seminal works [2, 3] opened the avenue to efficient algorithms for time-optimal robot motion along a specified geometric path, obtained by a non-uniform time scaling at different path points [5, 6].

*Work supported by MURST within the *MISTRAL* project.

On the other hand, robots using harmonic drives, long shafts, or belts as motion transmission elements are characterized by the presence of a dynamic displacement between the actuator positions and the link positions, usually modeled via elastic springs of finite stiffness [7]. More accurate Lagrangian models of robot dynamics have been derived, doubling the number of generalized coordinates and including the elasticity stored at the joints in the total potential energy [8]. Joint elasticity has a critical impact on the design of stabilizing control laws, as well as on dynamic-based trajectory planning [9].

In [3], a number of modifications were incorporated in the dynamic scaling algorithm, including velocity dependent actuator limits and joint viscous friction, but the additional presence of a position-dependent 'actuator springiness' was not carefully considered. At present, the only work dealing with the issue of optimal scaling of trajectories for elastic joint robots is [10]. The results therein are however limited to a single elastic degree of freedom with linear dynamics.

In this paper, we will show how to modify the uniform scaling algorithm of [3], in order to take into account joint elasticity in a general way. The dynamic model of robots with elastic joints is recalled in Sect. 2, together with its property of feedback linearizability and a limit analysis for infinite joint stiffness. The basic algorithm is presented in Sect. 3 for the case of absence of friction. In Sect. 4, the result is extended so as to include viscous friction at the joints. Numerical examples are reported in Sect. 5, considering a 2R planar robot with elastic joints moving in the presence or absence of gravity. Conclusions and further extensions are given in Sect. 6.

2 Robots with elastic joints

For an electrically-actuated robot with N joints undergoing elastic deformations, let $q \in \mathbb{R}^N$ be the link

0-7803-7272-7/02/$17.00 © 2002 IEEE

positions and $\theta \in \mathbb{R}^N$ be the motor positions, as reflected through the gear ratios [1]. The rotors of the motors are balanced uniform bodies, so that the inertia matrix and the gravity term in the dynamic model will be independent of θ. Following [8], we shall make an additional simplifying modeling assumption: the angular term of the kinetic energy of each rotor is only due to its relative rotation.

Using a Lagrangian approach, the robot dynamic model consists of $2N$ second-order differential equations:

$$M(q)\ddot{q} + c(q,\dot{q}) + F_q\dot{q} + g(q) + K(q-\theta) = 0 \quad (1)$$

$$J\ddot{\theta} + F_\theta\dot{\theta} + K(\theta - q) = u. \quad (2)$$

The symmetric inertia matrix $M(q) > 0$, the Coriolis and centrifugal vector $c(q,\dot{q})$ (quadratic in the velocity $\dot{q}$), the viscous friction diagonal matrix $F_q \geq 0$, and the gravity vector $g(q)$ are all related to the rigid links. The diagonal matrices $J > 0$, $F_\theta \geq 0$, and $K > 0$ contain, respectively, the effective motor inertias, the viscous friction coefficients at the motor side (both reflected through the gear ratio), and the joint stiffness constants, while $u \in \mathbb{R}^N$ are the motor torques.

We note that, in the limit case of infinite stiffness K, the following properties hold

$$\lim_{K\to\infty} \theta = q, \quad \lim_{K\to\infty} K(q-\theta) = \text{finite} \not\equiv 0,$$

and thus, by adding eqs. (1) and (2), the standard rigid robot model is obtained

$$(M(q) + J)\ddot{q} + c(q,\dot{q}) + (F_q + F_\theta)\dot{q} + g(q) = u. \quad (3)$$

The dynamic model (1–2) can be exactly transformed into a linear and input-output decoupled one via static state feedback [8]. This control property is crucial for the uniform scaling algorithm. In particular, we use the related property that the whole robot state $(q, \theta, \dot{q}, \dot{\theta}) \in \mathbb{R}^{4N}$ and the input torque u can be rewritten in terms of the link position vector q and its time derivatives up to the fourth order.

In fact, from eq. (1) it follows that θ can be written as a function of q, $\dot{q}$, and $\ddot{q}$. Differentiating eq. (1) w.r.t. time, and dropping functional dependence for compactness, yields

$$Mq^{[3]} + (\dot{M} + F_q)\ddot{q} + \dot{c} + \dot{g} + K(\dot{q} - \dot{\theta}) = 0, \quad (4)$$

where the notation $q^{[h]} = d^h q/dt^h$ has been used. Note that the dependence of $\dot{c}(q,\dot{q},\ddot{q})$ on $\ddot{q}$ and of $\dot{M}(q,\dot{q})$ and $\dot{g}(q,\dot{q})$ on $\dot{q}$ is linear. In addition, there is a cubic dependence of $\dot{c}$ on $\dot{q}$. From eq. (4), it follows that $\dot{\theta}$ can be explicitly written as a function of q, $\dot{q}$, $\ddot{q}$, and $q^{[3]}$. Differentiating eq. (4) w.r.t. time gives

$$Mq^{[4]} + (2\dot{M} + F_q)\ddot{q}^{[3]} + \ddot{c} + \ddot{M}\ddot{q} + \ddot{g} + K(\ddot{q} - \ddot{\theta}) = 0. \quad (5)$$

Again, the dependence of $\ddot{c}(q,\dot{q},\ddot{q},q^{[3]})$ on $q^{[3]}$ and of $\ddot{M}(q,\dot{q},\ddot{q})$ and $\ddot{g}(q,\dot{q},\ddot{q})$ on $\ddot{q}$ is linear. Eliminating $\dot{\theta}$ and $\ddot{\theta}$ from eq. (2), by using eqs. (4) and (5), and substituting from eq. (1)

$$K(\theta - q) = M\ddot{q} + c + F_q\dot{q} + g,$$

we finally obtain

$$\begin{aligned} u = \; & JK^{-1}\left[Mq^{[4]} + (2\dot{M} + F_q)\ddot{q}^{[3]} + \ddot{c} + \ddot{M}\ddot{q} + \ddot{g}\right] \\ & + F_\theta K^{-1}\left[Mq^{[3]} + (\dot{M} + F_q)\ddot{q} + \dot{c} + \dot{g}\right] \\ & + (M + J)\ddot{q} + c + (F_q + F_\theta)\dot{q} + g, \end{aligned} \quad (6)$$

which shows how the input torque u can be always expressed as a function of q, $\dot{q}$, $\ddot{q}$, $q^{[3]}$, and $q^{[4]}$. Therefore, the computation of a nominal torque $u(t)$ associated to a desired link motion $q(t)$ (inverse dynamics) can be performed in an algebraic way.

3 Uniform dynamic scaling

Assume that a robot trajectory has been defined in terms of link motions $q = q(t)$, for $t \in [0, T]$. In order to exactly reproduce $q(t)$, we also assume that: *i)* the desired motion is sufficiently smooth, i.e., $q(t)$ admits piecewise continuous fourth derivative w.r.t. time; *ii)* the initial robot state is matched with the boundary conditions of $q(t)$ (and its derivatives) at $t = 0$. In particular, for determining the required motor position $\theta(0)$ and velocity $\dot{\theta}(0)$, one should use eqs. (1) and (4).

Let the torques be bounded as $u \in [-U_M, U_M]$, where for simplicity we have assumed constant and symmetric actuator limits. For the given $q(t)$, the inverse dynamics (6) may result in unfeasible torques $u(t)$ or in an available margin of torque range. Accordingly, we wish to uniformly scale time t so as to obtain feasibility at all times and at least one time instants in which one or more torques are at their limits. Denote with

$$\tau = \frac{t}{\lambda}, \qquad \tau \in \left[0, \frac{T}{\lambda}\right] \quad (7)$$

the new time scale, with $0 < \lambda < 1$ for slower motion and $1 < \lambda < \infty$ for faster motion. In the new time scale, we have

$$\tilde{q}(\tau) = \tilde{q}\left(\frac{t}{\lambda}\right) = q(t), \quad (8)$$

[1] This coordinate definition allows to use the standard direct and inverse kinematics of the rigid arm in order to map link motion to end-effector cartesian motion and viceversa.

where a tilde denotes the new trajectory. Equation (8) expresses the fact that the same original sequence of link configurations (a path) is traced, but now at λ-scaled time instants. From eqs. (7–8), we have

$$\tilde{q}^{[h]} = \frac{d^h \tilde{q}}{d\tau^h} = \frac{d^h q}{dt^h}\left(\frac{dt}{d\tau}\right)^h = q^{[h]}\lambda^h, \quad h = 1, 2, \dots \quad (9)$$

We shall express the new inverse dynamics torque $\tilde{u}(\tau)$, for $\tau \in \left[0, \frac{T}{\lambda}\right]$, first in the frictionless case, i.e., $F_q = F_\theta = 0$. The original eq. (6) is then simplified and can be rearranged in the form

$$u(t) = A_4(t) + A_2(t) + g(q(t)), \quad (10)$$

with

$$\begin{aligned} A_4(t) &= JK^{-1}\Big[M(q(t))\,q^{[4]}(t) + 2\dot{M}(q(t),\dot{q}(t))\,q^{[3]}(t) \\ &\quad + \ddot{M}(q(t),\dot{q}(t),\ddot{q}(t))\,\ddot{q}(t) \\ &\quad + \dddot{c}(q(t),\dot{q}(t),\ddot{q}(t),q^{[3]}(t))\Big] \quad (11) \end{aligned}$$

$$\begin{aligned} A_2(t) &= (M(q(t)) + J)\,\ddot{q}(t) + c(q(t),\dot{q}(t)) \\ &\quad + JK^{-1}\ddot{g}(q(t),\dot{q}(t),\ddot{q}(t)). \quad (12) \end{aligned}$$

This grouping is made according to the homogeneity of differential orders of each term, respectively four in eq. (11) and two in eq. (12). For example, the ith component ($i = 1, \dots, N$) of the Coriolis and centrifugal vector has the structure

$$c_i(q,\dot{q}) = \frac{1}{2}\dot{q}^T C_i(q)\dot{q} = \frac{1}{2}\sum_j \sum_k c_{ijk}(q)\,\dot{q}_j\dot{q}_k,$$

where the elements $c_{ijk} = c_{ikj}$ of matrix C_i are Christoffel symbols (partial derivatives of the inertia matrix elements with respect to components of q). Differentiating c_i twice w.r.t. time, we obtain

$$\begin{aligned} \ddot{c}_i &= \tfrac{1}{2}\textstyle\sum_j\sum_k\sum_h\sum_\ell \frac{\partial^2 c_{ijk}}{\partial q_h \partial q_\ell}\dot{q}_j\dot{q}_k\dot{q}_h\dot{q}_\ell \\ &\quad + \tfrac{1}{2}\textstyle\sum_j\sum_k\sum_h \frac{\partial c_{ijk}}{\partial q_h}\left(\ddot{q}_h\dot{q}_j\dot{q}_k + 4\,\dot{q}_h\dot{q}_j\ddot{q}_k\right) \\ &\quad + \textstyle\sum_j\sum_k c_{ijk}\left(\ddot{q}_j\ddot{q}_k + \dot{q}_j q_k^{[3]}\right), \end{aligned}$$

where the sum of differential orders of each term is four. Therefore, $\dddot{c}$ appears in the A_4 term.

By using eqs. (8) and (9), we finally obtain for the new torque input

$$\begin{aligned} \tilde{u}(\tau) &= \tilde{A}_4(\tau) + \tilde{A}_2(\tau) + g(\tilde{q}(\tau)) \\ &= \lambda^4 A_4(t) + \lambda^2 A_2(t) + g(q(t)). \end{aligned} \quad (13)$$

This is the basic relation governing uniform time scaling of trajectories for elastic joint robots (in the absence of friction). The following remarks are in order.

- The rigid case is recovered for $K \to \infty$, since in the limit $A_4 = 0$ while A_2 reduces to the inertial, Coriolis and centrifugal terms of the rigid dynamics (3). The quadratic scaling of torques by λ^2 is thus obtained, up to the gravity term, as in [3].
- For decreasing $\lambda << 1$ (very slow motion), the fourth order term in eq. (13), including the main dynamic effects of joint elasticity, becomes negletable with respect to the quadratic term. This is in accordance with intuition, since sufficiently slow motion does not excite vibrational behavior. However, in comparison with the rigid case, there is an additional contribution in the quadratic term ($\ddot{g}$) which may be still relevant. On the other hand, the complex fourth order term is the dominant factor for increasing $\lambda >> 1$ (very fast motion).
- Differently from the rigid case [3], time scaling may also change the sign of the needed torque at one point along the path. This occurs when the signs of $A_4(t)$ and $A_2(t)$ are opposite.
- Equation (13) indicates that, during inverse dynamics computation along an initial trajectory, it is wise to store separately the three vector components of the total torque A_4, A_2, and g. In the absence of gravity, A_2 is exactly the torque needed for a rigid robot dynamic model.

We conclude this section with the algorithm for determining all feasible scaling of trajectories that satisfy torque limitations. As in [3], define the following upper and lower bounds for the torques, local to each path point

$$U^-(t) = -U_M - g(q(t)), \quad U^+(t) = U_M - g(q(t)). \quad (14)$$

The scaled torque $\tilde{u}(\tau)$ will be feasible iff λ satisfies the following two vector inequalities

$$U^-(t) \le \lambda^4 A_4(t) + \lambda^2 A_2(t) \le U^+(t), \quad (15)$$

for $t \in [0, T]$. The algorithm uses the biquadratic structure of the inequalities in (15). Let $\mu = \lambda^2$.

Scaling Algorithm

1. For each $i \in \{1, \dots, N\}$ and $t \in [0, T]$, solve in closed form the two scalar quadratic equations

$$\begin{aligned} \mu^2 A_{4,i}(t) + \mu\, A_{2,i}(t) - U_i^-(t) &= 0 \quad (16) \\ \mu^2 A_{4,i}(t) + \mu\, A_{2,i}(t) - U_i^+(t) &= 0. \quad (17) \end{aligned}$$

Consider only the positive real roots of eqs. (16) and (17), which may be two ($0 < \mu_1^{-/+} < \mu_2^{-/+}$), one ($0 < \mu_1^{-/+}$), or none for each equation.

2. Analyze the sign of $\Delta^- = 2A_{4,i}(t)\mu_1^- + A_{2,i}(t)$. If eq. (16) has two positive real roots, the associated feasible interval $\Lambda^-(i,t)$ for λ is determined as:

$$\Delta^- > 0 \quad \Rightarrow \quad \lambda \in \left[\sqrt{\mu_1^-}, \sqrt{\mu_2^-}\right]$$

$$\Delta^- < 0 \quad \Rightarrow \quad \lambda \in \left(0, \sqrt{\mu_1^-}\right] \bigcup \left[\sqrt{\mu_2^-}, \infty\right).$$

If eq. (16) has only one positive real root, then:

$$\Delta^- > 0 \quad \Rightarrow \quad \lambda \in \left[\sqrt{\mu_1^-}, \infty\right)$$

$$\Delta^- < 0 \quad \Rightarrow \quad \lambda \in \left(0, \sqrt{\mu_1^-}\right].$$

Perform a similar analysis on the sign of $\Delta^+ = -(2A_{4,i}(t)\mu_1^+ + A_{2,i}(t))$, in association with eq. (17) and derive the feasible interval $\Lambda^+(i,t)$. Define $\Lambda(i,t) = \Lambda^-(i,t) \cap \Lambda^+(i,t)$.

3. Feasible uniform time scaling constants λ satisfy

$$\lambda \in \Lambda = \bigcap_{i=1,\ldots,N} \bigcap_{t\in[0,T]} \Lambda(i,t) \subseteq I\!R^+$$

■

For simplicity, we have not detailed some special cases that may occur in steps 1–2 (no real positive roots, two coincident positive real roots). They either lead to an empty $\Lambda(i,t)$ or do not contribute in its definition, depending on the sign of terms in inequalities (15). The set Λ may result in a single interval, in multiple disjoint intervals, or be empty. Indeed, an empty (intermediate or final) interval implies that no uniform time scaling is able to guarantee torque feasibility. If $\Lambda \neq \emptyset$, the locally optimal time $T_{\text{opt}} = T/\lambda_{\text{opt}}$ along the given path is obtained by choosing $\lambda_{\text{opt}} = \sup \Lambda$.

4 Inclusion of viscous friction

We turn back to the case of presence of viscous friction in the model (1–2) and indicate only the main differences that arise with respect to the analysis of Sect. 3.

For $F_q \not\equiv 0$ and/or $F_\theta \not\equiv 0$, the inverse dynamics computation (6) can be arranged in the form

$$u_F(t) = A_{4F}(t) + A_{3F}(t) + A_{2F}(t) + A_{1F}(t) + g(q(t)), \tag{18}$$

where the terms

$$A_{4F}(t) = A_4(t)$$

$$A_{3F}(t) = F_\theta K^{-1}\left[M(q(t))q^{[3]}(t) + \dot{M}(q(t),\dot{q}(t))\ddot{q}(t) + \dot{c}(q(t),\dot{q}(t),\ddot{q}(t))\right] + JK^{-1}F_q\, q^{[3]}(t)$$

$$A_{2F}(t) = A_2(t) + F_\theta K^{-1} F_q\, \ddot{q}(t)$$

$$A_{1F}(t) = (F_q + F_\theta)\,\dot{q}(t) + F_\theta K^{-1}\dot{g}(q(t),\dot{q}(t))$$

are grouped with respect to their homogeneity of differential order. In place of eq. (13), we will obtain

$$\tilde{u}_F(\tau) = \sum_{h=1}^{4} \lambda^h A_{hF}(t) + g(q(t)). \tag{19}$$

The occurrence of a complete quartic polynomial equation requires a suitable modification of steps 1–2 in the Scaling Algorithm. The basic outcome of the analysis is summarized in Table 1, where $0 < \lambda_1 < \ldots < \lambda_k$ are the k real positive roots ($k \in \{0,\ldots 4\}$) of either one of the equations associated with the two scalar inequalities

$$U_i^-(t) \leq \sum_{h=1}^{4} \lambda^h A_{hF,i}(t) \leq U_i^+(t),$$

for $i = 1,\ldots,N$. The cases are discriminated w.r.t. the sign of $\Delta_F^- = \sum_{h=1}^4 h\left(\lambda_1^-\right)^{h-1} A_{hF,i}(t)$ (or of the analogous Δ_F^+).

k	$\Delta_F^{-/+} > 0$	$\Delta_F^{-/+} < 0$
1	$\left[\lambda_1, +\infty\right)$	$\left(0, \lambda_1\right]$
2	$\left[\lambda_1, \lambda_2\right]$	$\left(0, \lambda_1\right] \bigcup \left[\lambda_2, +\infty\right)$
3	$\left[\lambda_1, \lambda_2\right] \bigcup \left[\lambda_3, +\infty\right)$	$\left(0, \lambda_1\right] \bigcup \left[\lambda_2, \lambda_3\right]$
4	$\left[\lambda_1, \lambda_2\right] \bigcup \left[\lambda_3, \lambda_4\right]$	$\left(0, \lambda_1\right] \bigcup \left[\lambda_2, \lambda_3\right] \bigcup \left[\lambda_4, +\infty\right)$

Table 1: Possible structures of the feasible interval $\Lambda(i,t)$, in the presence of viscous friction (k is the number of positive real roots)

5 Numerical results

We have performed several numerical tests of the scaling algorithm (written in MATLAB) for various elastic joint robots with different parameters [11]. Here, we report results for a planar lightweight 2R robot with the following data: for each link, length = 0.5 m, uniformly distributed mass = 1 kg, inertia w.r.t. joint axis = 0.0215 kg·m^2; for each motor, mass = 0.1 kg, inertia reflected through the gear ratio = 0.05 kg·m^2, and transmission stiffness = 100 Nm.

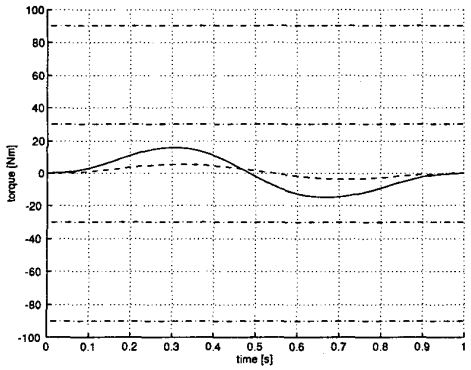

Figure 1: Torques before scaling in case I: joint 1 (−), joint 2 (- -)

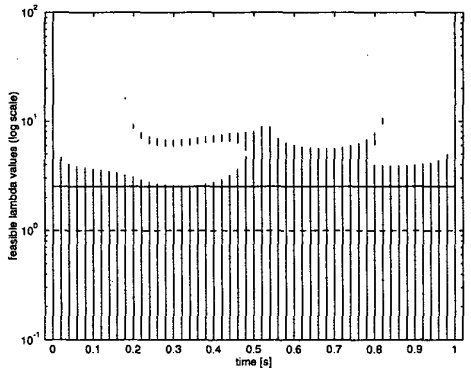

Figure 2: Intervals $\Lambda(2,t)$, $t \in [0,1]$, in case I

Case I In this case, there is no friction and the arm moves in the horizontal plane (no gravity). The torque limits are set to $U_{M1} = 90$ Nm and $U_{M2} = 30$ Nm. the reference trajectory is

$$q(t) = q_0 + (q_f - q_0)s(t), \quad t \in [0,T], \qquad (20)$$

where $s(t)=126\left(\frac{t}{T}\right)^5-420\left(\frac{t}{T}\right)^6+540\left(\frac{t}{T}\right)^7-315\left(\frac{t}{T}\right)^8+70\left(\frac{t}{T}\right)^9$ is chosen so as to satisfy zero boundary conditions for the first four time derivatives of $q(t)$ at time $t = 0$ and $t = T$. Let $q_0 = (-90°, 0°)$ and $q_f = (30°, 60°)$, and assume initially $T = 1$ s.

The torques needed for the original motion are shown in Fig. 1, indicating feasibility for both joints. The feasible intervals $\Lambda(1,t)$ and $\Lambda(2,t)$ are computed by the Scaling Algorithm, using 51 sampled instants $t \in [0,T]$. Figure 2 shows the result for the second joint ($i = 2$), using a logarithmic scale; an horizontal straight line denotes the feasible scaling limit. The final scaling interval $\Lambda = (0, 2.530]$ indicates that the motion can be considerably speeded up. The torques

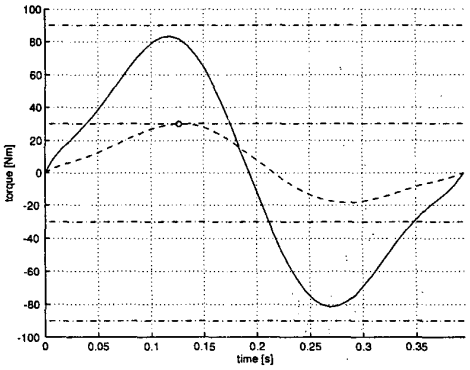

Figure 3: Torques after scaling by $\lambda = 2.530$ in case I: joint 1 (−), joint 2 (- -)

obtained for a total motion time $T_{\text{opt}} = T/2.530 = 0.395$ s are shown in Fig. 3. If time scaling was performed assuming rigid joints, the feasible scaling interval would have been $(0, 2.330]$, with an increase of the shortest achievable time of about 9%. Thus, elasticity works in favour of speed.

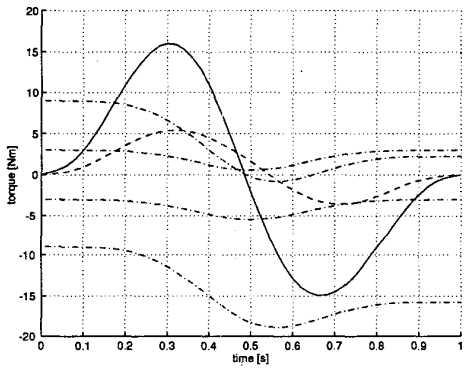

Figure 4: Torques before scaling in case II: joint 1 (−), joint 2 (- -)

Case II We include gravity and reduce the torque limits to $U_{M1} = 9$ Nm and $U_{M2} = 3$ Nm. The original unfeasible torques are reported in Fig. 4, up to gravity components: the dashed-dotted lines are the time-varying bounds $U^-(t)$ and $U^+(t)$ defined in eq. (14). The Scaling Algorithm yields a feasible interval $\Lambda = [0.343, 0.474]$, with lower bound induced by joint 1 (see Fig. 5) and upper bound by joint 2. Thus, feasible motion time varies between $T_{\text{opt}} = T/0.474 = 2.109$ s, with joint 2 saturation (Fig. 6), and $T_{\max} = T/0.343 = 2.913$ s, with joint 1 (Fig. 7) saturation. Time scaling performed with rigid joints gives the slightly reduced feasible interval $[0.348, 0.466]$.

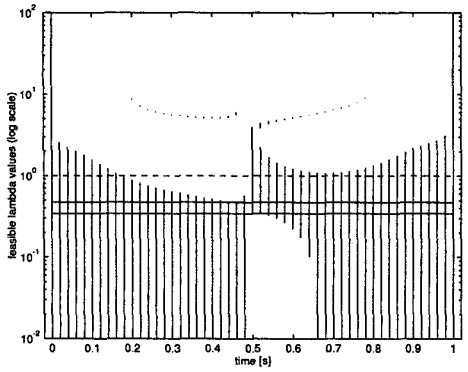

Figure 5: Intervals $\Lambda(1,t)$, $t \in [0,1]$, in case II

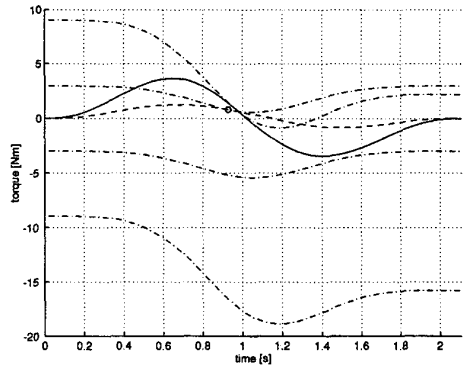

Figure 6: Torques after scaling by $\lambda = 0.474$ in case II: joint 1 (−), joint 2 (- -)

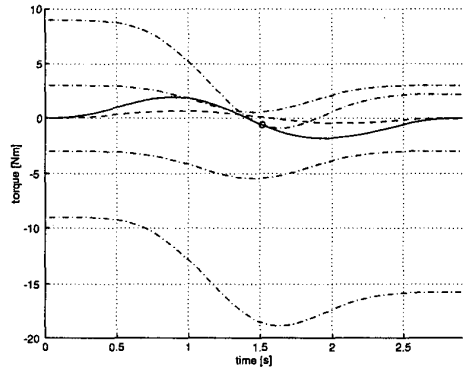

Figure 7: Torques after scaling by $\lambda = 0.343$ in case II: joint 1 (−), joint 2 (- -)

Case III Consider a constant link velocity motion from $q_0 = 0$ to $q_f = (10°, 60°)$ without gravity. Friction is included, with all coefficients set to 0.005 Nms. Torque limits are $U_{M1} = 12$ Nm and $U_{M2} = 3$ Nm.

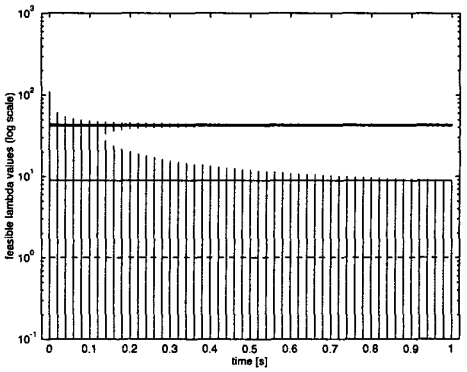

Figure 8: Intervals $\Lambda(1,t)$, $t \in [0,1]$, in case III

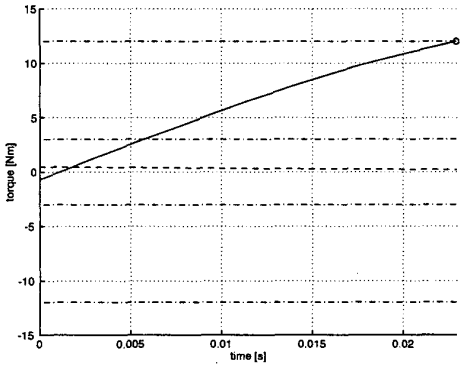

Figure 9: Torques after scaling by $\lambda = 43.572$ in case III: joint 1 (−), joint 2 (- -)

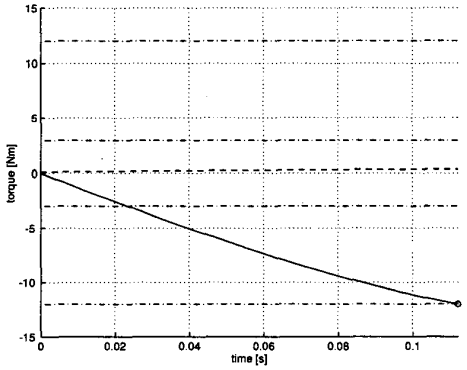

Figure 10: Torques after scaling by $\lambda = 8.907$ in case III: joint 1 (−), joint 2 (- -)

The original torques are largely feasible for $T = 1$ s.

The modified algorithm of Sect. 4 provides

$$\bigcap_{t\in[0,1]} \Lambda(1,t) = (0, 8.907] \cup [41.805, 43.572]$$
$$\bigcap_{t\in[0,1]} \Lambda(2,t) = (0, 50.822],$$

so that Λ is fully specified by the first joint. In this case, see Fig. 8, it is notable the presence of a small 'island' of admissible scaling parameters, that corresponds to a motion at a very high constant speed, not allowed in the equivalent rigid case. Figures 9 and 10 show the torque profiles for the shortest total time $T_{\text{opt}} = 1/43.572 \approx 0.02$ s and, respectively, the more conventional solution $\lambda = 8.907$ leading to a traveling time of about 0.11 s.

6 Conclusions

A detailed analysis of the dynamic scaling property of trajectories in robots with elastic joints has been presented. We have given an algorithm for determining the uniform scaled time intervals that lead to feasible torques (with saturation in at least one instant). This basically involves the solution of biquadratic equations, and of complete quartic polynomial equations in the additional presence of viscous friction. For elasticity going to infinity, the original results valid for rigid manipulators are recovered.

Joint elasticity modifies the limits of feasible time scaling, and sometimes also its structure, and allows motion at faster speed. The physical explanation is that the elastic moments acting on the links through the joint transmissions may become (typically for a short transient period) even larger than the bounds set on the actuator torques. The particular case of trajectories with constant link velocity leads to the existence of critical solutions, implying very fast motion. More in general, the incidence of these modifications depends on the total available torque, on the actual joint stiffness, as well as on the gear reduction and motor-to-link inertia ratio.

We are currently extending the dynamic scaling approach also to the case of robots with visco-elastic joints and of robots with flexible links. The use of non-uniform time scaling for determining a time optimal solution along a given geometric path is still an open problem for robots with flexible elements.

References

[1] L. Sciavicco and B. Siciliano, *Modeling and Control of Robot Manipulators*, McGraw-Hill, New York, 1996.

[2] J. E. Bobrow, *Optimal Control of Robotic Manipulators*, Ph.D. Thesis, University of California, Los Angeles, 1982.

[3] J. M. Hollerbach, "Dynamic scaling of manipulator trajectories," *ASME J. of Dynamic Systems, Measurement, and Control*, vol. 106, pp. 102–106, 1984.

[4] J. Y. S. Luh, M. W. Walker, and R. P. C. Paul, "On-line computational scheme for mechanical manipulators," *ASME J. of Dynamic Systems, Measurement, and Control*, vol. 102, pp. 69–76, 1980.

[5] K. Shin and N. D. McKay, "Minimum-time control of robotic manipulators with geometric path constraints," *IEEE Trans. on Automatic Control*, vol. 30, no. 6, pp. 531–541, 1985.

[6] J. E. Bobrow, S. Dubowsky, and J. S. Gibson, "Time-optimal control of robotic manipulators along specified paths," *Int. J. of Robotics Research*, vol. 4, no. 3, pp. 3–17, 1985.

[7] M. C. Good, L. M. Sweet, and K. L. Strobel, "Dynamic models for control system design of integrated robot and drive systems," *ASME J. of Dynamic Systems, Measurement, and Control*, vol. 107, pp. 53–59, 1985.

[8] M. W. Spong, "Modeling and control of flexible joint robots," *ASME J. of Dynamic Systems, Measurement, and Control*, vol. 109, pp. 310–319, 1987.

[9] A. De Luca and P. Tomei, "Elastic joints," in *Theory of Robot Control*, C. Canudas de Wit, B. Siciliano, G. Bastin (Eds.), pp. 179–217, Springer Verlag, Berlin, 1996.

[10] O. Dahl, "Path constrained robot control," Ph. D. thesis, Dept. of Automatic Control, Lund Institute of Technology, 1992.

[11] R. Farina, "Dynamic scaling of trajectories for robots with flexible elements," Laurea thesis (in Italian), Dip. di Informatica e Sistemistica, Università di Roma "La Sapienza", 2001.